Cysteine Scanning of MscL Transmembrane Domains Reveals Residues Critical for Mechanosensitive Channel Gating

Gal Levin and Paul Blount
Department of Physiology, University of Texas-Southwestern Medical Center, Dallas, Texas

ABSTRACT The mechanosensitive channel of large conductance (MscL), a bacterial channel, is perhaps the best characterized mechanosensitive protein. A structure of the *Mycobacterium tuberculosis* ortholog has been solved by x-ray crystallography, but details of how the channel gates remain obscure. Here, cysteine scanning was used to identify residues within the transmembrane domains of *Escherichia coli* MscL that are crucial for normal function. Utilizing genetic screens, we identified several mutations that induced gain-of-function or loss-of-function phenotypes in vivo. Mutants that exhibited the most severe phenotypes were further characterized using electrophysiological techniques and chemical modifications of the substituted cysteines. Our results verify the importance of residues in the putative primary gate in the first transmembrane domain, corroborate other residues previously noted as critical for normal function, and identify new ones. In addition, evaluation of disulfide bridging in native membranes suggests alterations of existing structural models for the "fully closed" state of the channel.

INTRODUCTION

The ability to detect mechanical force underlies many normal biological processes including the senses of hearing and balance, tissue development, and osmotic regulation. The sensors able to detect these forces often appear to be mechanosensitive (MS) channels (Hamill and Martinac, 2001). However, little is known of the molecular mechanisms of this large class of channels.

The first gene shown to encode an MS channel activity was *mscL*, the mechanosensitive channel of large conductance from *Escherichia coli* (Sukharev et al., 1994). The encoded 136-amino acid protein has been shown to be essential as well as sufficient for one of the primary mechanosensitive channel activities observed in bacterial membranes (Häse et al., 1995; Blount et al., 1996a). MscL opens a large pore, an estimated 30 Å in diameter (Cruickshank et al., 1997), in response to membrane tension. The channel conducts ions, and passes other solutes including some proteins (Ajouz et al., 1998; Berrier et al., 2000). MscL appears to play a key role in bacterial osmoregulation. *E. coli* cells null for MscL and another primary MS channel, the mechanosensitive channel of small conductance (MscS), are particularly sensitive to hypoosmotic shock. Restoring expression of either mechanosensitive channel rescues this osmotic-fragile phenotype (Levina et al., 1999; Moe et al., 2000). In wild-type bacteria, it appears that the opening of MscS is the initial response to a hypoosmotic shock. MscL is activated in larger osmotic gradients, when membrane tension approaches lysis (Berrier et al., 1996). Early membrane topology studies suggested that a MscL subunit contains two transmembrane domains (TM1 and TM2), a periplasmic loop, and cytoplasmic N- and C-termini (Blount et al., 1996a). The subsequent crystallization and structural resolution to 3.5 Å of the *Mycobacterium tuberculosis* ortholog (Chang et al., 1998) supported the topological analysis of *E. coli* MscL and clarified that the functional channel is a homopentamer. In addition, the structure showed the transmembrane helices tilting slightly, and the TM1 bundles converging to form a constriction point of ~4 Å. The authors noted that the structure most likely represents a closed or ''nearly closed'' state of the molecule.

Studies utilizing random and site-directed mutagenesis have identified several residues required for the normal function of this mechanosensitive channel (Blount et al., 1996b, 1997; Ou et al., 1998; Yoshimura et al., 1999; Maurer et al., 2000; Kumánovics et al., 2002; Maurer and Dougherty, 2003). In one of the first studies (Ou et al., 1998), randomly mutated *mscL* was placed under the transcriptional control of an inducible promoter. Cells that showed a slowed or no-growth phenotype when the mutant MscL was expressed in an MscL-null strain were isolated. Because the null, with or without expression of wild-type channels, did not exhibit such a phenotype, the mutants isolated are gain-of-function (GOF). The majority of mutations were in TM1. Further characterization of the mutated channels suggested that the phenotype was a result of channels that gated at lower tension. More recently, a high-throughput screen was utilized to characterize 348 *E. coli* MscL mutants created randomly (Maurer and Dougherty, 2003). This study confirmed the importance of TM1 for function of the channel, extended our knowledge of critically important residues in other domains, and expanded previous findings by identifying mutations that led to nonfunctional proteins, several of which were found in the TM2 and the periplasmic loop. Note, however, that the random mutagenesis studies can be biased in interpretation because some

Submitted November 4, 2003, and accepted for publication January 8, 2004.
Address reprint requests to Paul Blount, Dept. of Physiology, University of Texas-Southwestern Medical Center, 5323 Harry Hines Blvd., Dallas, TX 75390-9040. Tel.: 214-648-8445; Fax: 214-648-4771; E-mail: Paul.Blount@UTSouthwestern.edu.

0006-3495/04/05/2862/09 $2.00

codons have a higher probability, upon a single base change, of encoding nonconservative substitutions. A more systematic approach scans an entire region of the protein by substituting each residue, sequentially, with a residue that would not be likely to lead to large disruptions in protein conformation.

Cysteine scanning has been utilized previously to determine functional regions within transmembrane domains (Lee et al., 1995). Here, we have used this approach to determine residues in TM1 and TM2 that play important roles in the gating of MscL. Cysteine is an appropriate choice for scanning such domains because its hydrophobicity lies near the middle range for transmembrane residues and its relatively small size means that perturbation of packing interfaces would likely be subtle. In addition, it is found in every protein secondary structure and is therefore unlikely to distort global structure. Hence, when a cysteine substitution does lead to phenotypic changes in a gated channel, it suggests that some feature of the substituted residue (e.g., size, hydrophilicity, aromatic ring, or charge) is important for normal channel function. Furthermore, cysteine has the advantage that it may form intercysteine disulfide bridges, thus serving to determine the proximity of residues of the pentamer (e.g., determine pore constriction points); if the proteins are never detergent solubilized, it is likely that the findings reflect a stable conformation in native membranes. Utilizing this approach, combined with whole-cell physiological and electrophysiological methods, we confirm the importance of TM1, and implicate the participation of TM2, in MscL gating. The data suggest modifications of current models for the structure of the fully closed conformation of the channel, as well as help to resolve conflicts between current hypotheses for the mechanisms of MscL gating.

MATERIALS AND METHODS

Strains and cell growth

E. coli strain PB104 (Δ*mscL::*Cm) (Blount et al., 1996a), was used to host the pB10 expression constructs (Blount et al., 1996a; Ou et al., 1998; Moe et al., 2000) for GOF and electrophysiological analysis. Similarly, the *E. coli* FRAG-1 (Epstein and Davies, 1970) derivative strain, MJF455 Δ*mscL::*Cm, Δ*yggB* (Levina et al., 1999), was used as host for the suppression of the lysis phenotype assay. Cultures were routinely grown in Lennox Broth (LB) plus ampicillin (100 μg/ml) in a shaker-incubator at 37°C, rotated 250 cycles/min. For Western analysis, K10 minimal medium was used (Epstein and Kim, 1971): 46 mM Na_2HPO_4, 23 mM NaH_2HPO_4, 8 mM $(NH_4)_2SO_4$, 0.4 mM $MgSO_4$, 6 μM $FeSO_4$, 1 μg/ml thiamine, 100 μg/ml of the amino acids histidine, leucine, threonine, valine, and isoleucine, 0.2% glucose, 10 mM KCl, and 100 μg/ml ampicillin. Expression was induced by addition of isopropyl β-D-thiogalactopyranoside (IPTG; 1 mM).

Mutagenesis

Site-directed mutagenesis of *mscL* was accomplished by polymerase chain reaction, using either a QuikChange site-directed mutagenesis kit (Stratagene, La Jolla, CA) or a modified megaprimer protocol: briefly, oligonucleotide primers were designed that incorporated the desired codon change accompanied by two 12- to 18-base pair flanking sequences on each side. The final product was created in a two-stage reaction using a wild-type MscL in pBluescript II (Stratagene) as a template. For creating mutations in TM1, the first stage used the mutating primer in conjunction with the 5′ primer (containing T3 polymerase consensus) to generate a megaprimer. The second reaction incorporated the megaprimer and the 3′ primer (containing T7 polymerase consensus) to yield a full-length final product. Mutations in TM2 were generated similarly, except that the mutating primer was of the complementary sequence, the first step was performed in conjugation with the 3′ primer, and the second step utilized the resulting megaprimer and the 5′ primer. The full-length product, ligated into pBluescript, was sequenced in both directions to verify the single mutation. The mutated MscL was then subcloned into the pB10b expression vector utilizing either of the set of restriction enzyme consensus site pairs *Xba*I/*Sal*I or *Xba*I/*Xho*I (Blount et al., 1996a,b). Successful subcloning and final verification of the mutation was ascertained by sequencing through the mutation. The codon used for cysteine was TGC except for G22C, a generous gift from Professor Kung, which used TGT.

In vivo assays: GOF and suppression of the osmotic lysis phenotype

For the GOF assays, a single colony was used to inoculate two 10-ml cultures of LB plus ampicillin (100 μg/ml), one of which was supplemented with 1 mM IPTG. Cultures were grown for 17–19 h, and then an optical density $(OD)_{600}$ of both cultures was measured and compared. All experiments were performed at least three times and reflect consistent results from at least two independently transformed colonies.

To assay for suppression of the osmotic lysis phenotype, a single colony was used to inoculate a culture of LB plus ampicillin. The cells were grown to OD_{600} 0.35–0.55; the culture was then combined with an equal volume of prewarmed (37°C) LB supplemented with 100 μg/ml ampicillin, 2 mM IPTG, and 1 M NaCl (making the final concentrations 1 mM IPTG and 500 mM NaCl) and grown for an additional 1 h. As previously described (Moe et al., 2000), hypotonic shock was applied by a 1000-fold dilution into sterile ddH_2O for 20 min at 37°C, while the control was similarly diluted into the isotonic LB medium (above), without IPTG. Viability following the osmotic shock was assessed by viable plate count on LB/ampicillin plates.

Electrophysiology

E. coli giant spheroplasts were generated and used in patch-clamp experiments as described previously (Blount and Moe, 1999). Excised, inside-out patches were examined at room temperature under symmetrical conditions using a buffer comprised of 200 mM KCl, 90 mM $MgCl_2$, 10 mM $CaCl_2$, and 5 mM HEPES adjusted to pH 6.0. Recordings were performed at −20 mV. Data were acquired at a sampling rate of 20 kHz with a 5 kHz filter using an AxoPatch 200B amplifier in conjunction with Axoscope software (Axon Instruments, Union City, CA). A piezoelectric pressure transducer (World Precision Instruments, Sarasota, FL) was used to measure the pressure throughout the experiments. The tension sensitivity was determined by dividing MscL pressure threshold with that of MscS, as previously described (Blount et al., 1996b, 1999; Ou et al., 1998). For experiments utilizing dithiothreitol (DTT) (Sigma, St. Louis, MO), 1–5 mM final concentration was added to the bath after seal formation and MscS activity had been established; effects were observed within 3 min of treatment. Alternatively, where indicated, DTT was added to the pipette solution.

Western blot analysis

PB104 *E. coli* were grown in K10 minimal medium to log phase (OD_{600} 0.3–0.5), then 1 mM IPTG was added and the cells were grown for an additional 30 min. EDTA (1 mM) was then added, and half of the culture

was treated with 100 mM DTT. After 1–2 h of additional incubation and rotation at 37°C, the cells were collected by centrifugation and frozen at −80°C until sodium dodecyl sulfate polyacrylamide gel electrophoresis (SDS-PAGE) analysis. Cell pellets were suspended in nonreducing Laemmli buffer (62.5 mM Tris, pH 6.8, 25% v/v glycerol, 2% w/v SDS, 0.01% w/v bromophenol blue) heated to 70°C for 4 min, and fractionated on a 10–20% gradient SDS polyacrylamide gel (Bio-Rad, Hercules, CA). Proteins were electrotransferred to a polyvinylidene difluoride membrane and the Western blot analysis was performed using primary antibodies against the MscL C-terminus as previously described (Blount et al., 1996b) and an Immuno-Star Chemiluminescent Protein Detection System (Bio-Rad) according to the manufacturer's instruction. To eliminate nonspecific binding, the antibodies were preabsorbed with PB104 (MscL null) cell lysate prior to use and IgG was purified using ImmunoPure immobilized Protein A/G kit (Pierce, Rockford, IL). X-ray film was exposed to the blotted membrane. The developed film was scanned and then processed using CorelDRAW software (Corel Graphics, Ottawa, Canada).

RESULTS

Several MscL channels with cysteine substitutions do not function normally in vivo

As described in Materials and Methods, 62 cysteine-substitution mutants were generated in the two transmembrane domains of MscL: TM1 (R13–M42) and TM2 (A70–K101). A graphic representation of the regions of the MscL protein that were targeted is shown in Fig. 1, which shows

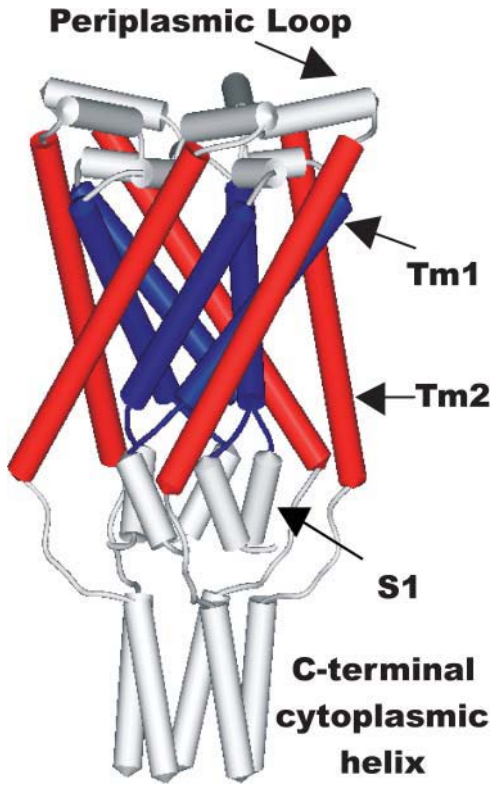

FIGURE 1 A schematic depiction of *E. coli* MscL and the domains that were targeted for substitutions. Shown is a proposed model for a closed conformation of the *E. coli* MscL homopentamer (Sukharev et al., 2001b) that is largely based upon a crystal structure of the *M. tuberculosis* ortholog (Chang et al., 1998). The targeted area in TM1 is colored blue, TM2 in red.

a proposed model for the closed structure of the *E. coli* MscL (Sukharev et al., 2001b) that is largely based upon a crystal structure of the *M. tuberculosis* ortholog (Chang et al., 1998). All mutated genes were subcloned into the pB10b expression vector and expressed in the *mscL*-null *E. coli* strain PB104 (Blount et al., 1996a; Ou et al., 1998; Moe et al., 2000). This transformed strain was subsequently assayed for phenotypic changes. Previous studies have shown that MscL mutants that gate at a lower tension threshold can cause the cell to enter stationary phase prematurely (Yoshimura et al., 1999; Moe et al., 2000). We found that measuring the early stationary OD_{600} provided a GOF assay that was simple, easy to quantitate, and extremely sensitive when compared to determination of growth rates or plate phenotypes. As shown in Fig. 2 *A*, all but nine of the 62 cysteine-substitutions effect some GOF phenotype by this criterion. Seventeen mutants achieved only 50% or less of uninduced stationary OD, or fell within two SEM of this value; we defined these mutants as strong GOF phenotypes. Viability plate assays demonstrated that this reduction in OD reflects a true decrease in the number of viable cells rather than a change in optical properties of the cells (not shown).

We further screened the library for the ability to suppress an osmotic phenotype previously reported (Levina et al., 1999; Moe et al., 2000). Briefly, we used an *E. coli* strain that lacks both primary mechanosensitive channels, MscL and MscS, and thus is exceptionally sensitive to osmolarity, losing viability when challenged by an acute decrease in osmotic environment. For simplicity, we will refer to this fragility as the ''osmotic-lysis phenotype.'' Expression of wild-type MscS in *trans*, in which the plasmid utilized the endogenous promoter, was shown to rescue this phenotype (Levina et al., 1999). Subsequent studies demonstrated that expression of either MscS (Okada et al., 2002) or MscL (Moe et al., 2000) in *trans* using an IPTG-inducible promoter also rescues the phenotype. Channels that function normally, therefore, suppress the osmotic-lysis phenotype; presumably, nonfunctional channels would not. As a first approximation, mutant MscS or MscL channels that do not suppress the osmotic lysis phenotype could be considered as loss-of-function (LOF). It should be noted, however, that this method may suggest erroneous interpretations if the mutation effects a GOF phenotype. For example, decreased cell turgor due to solutes leaking through a partially open pore may give the appearance of a normally functioning channel by this assay, even if the channel is no longer gated by membrane tension. Alternatively, stresses resulting from a GOF phenotype may be compounded by the osmotic shock, or the cell may overcompensate upon osmotic shock, thus leading to a decrease in viability that is scored as a LOF. Indeed, three mutations (V21C, V33C, and V37C) that effect a strong GOF phenotype and were shown to encode a channel with increased tension sensitivity relative to wild-type, failed to suppress the osmotic-lysis phenotype (not shown). Because of this potential complication in interpretation, we

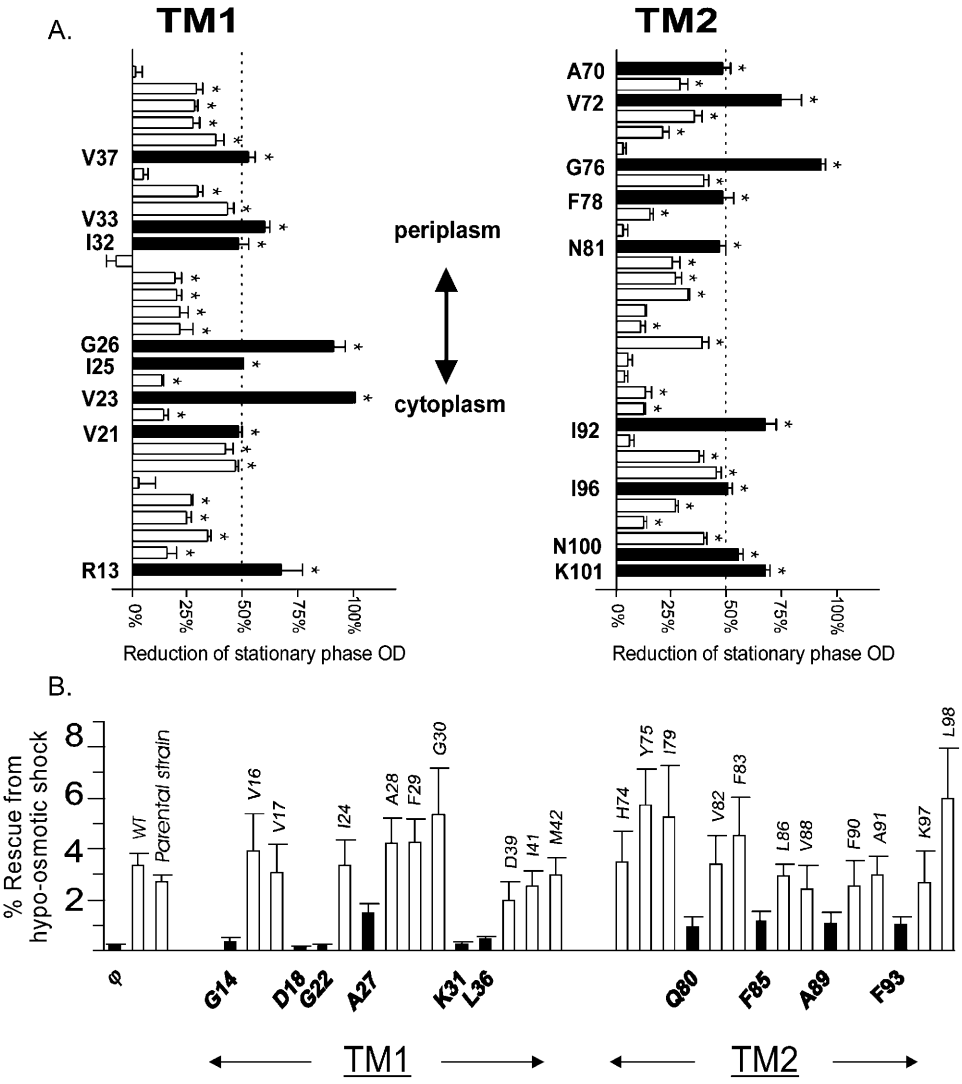

FIGURE 2 Some MscL mutants do not function normally in vivo. (*A*) GOF phenotype in growth assay. Shown is the extent of reduction in OD_{600} of stationary LB culture (average ± SE, $n \geq 3$). *$p < 0.005$, compared to the wild-type strain. The dashed line at 50% demarcates the threshold used to identify severe GOF mutants, which are labeled to the left of the filled bars. (*B*) LOF phenotype assay. Mutants that exhibited ≤25% inhibition of growth were tested for their ability to remediate the osmotic-lysis phenotype of *E. coli* MJF455. Shown is the effect of osmotic shock on viability. Filled bars and labels at the bottom of the graph indicate mutants that failed to rescue MJF455 cells from hypoosmotic shock as compared to wild-type MscL, thus exhibiting a LOF phenotype. *$p < 0.05$. The pB10 expression plasmid, not containing *mscL*, is shown as a control (labeled Φ).

present data only for mutants that exhibit 25% or less decrease in growth in the GOF assay discussed above and shown in Fig. 2 *A*. Of these 30 mutants, 10 showed a significant decrease in their ability to suppress the osmotic-lysis phenotype (Fig. 2 *B*).

Electrophysiological analysis of mutants

All mutations that effect either a strong GOF or LOF phenotype were characterized by patch clamp. As described previously, giant spheroplasts were generated, and MscS activity was used as an internal control to determine the tension threshold sensitivity (Blount et al., 1996b, 1999; Ou et al., 1998). Seals of >4 GΩ were obtained for all mutants examined, suggesting that all of the mutants were in a closed state before a pressure stimulus was applied.

Fourteen of 17 GOF mutants encoded easily identifiable MscL activity (Fig. 3). Twelve of these mutants had a lower sensitivity threshold (Table 1), as has been previously observed for channels effecting similar phenotypes (Ou et al., 1998; Yoshimura et al., 1999). Previous studies found that GOF mutants often exhibit decreased open dwell times, leading to a channel that appears ''flickery.'' Consistent with those studies, we found that all 12 mutants encoded channels with shorter open dwell times (Table 1). The two exceptions, mutations A70C and V72C, which are at the periplasmic end of TM2, showed neither increased sensitivity nor decreased open dwell times.

Similar electrophysiological characterization was performed with mutants that did not suppress the osmotic-lysis phenotype (Fig. 2 *B*). Eight of 10 of these mutants encoded channels that either required significantly higher membrane tension to gate or were not normally detected before rupture of the membrane patch (Fig. 3, Table 2). One trivial explanation for the lack of detection of some mutants could be decreased expression. However, Western blot analysis suggests that these channels have expression levels greater than or equal to wild-type controls (not shown). Hence, the

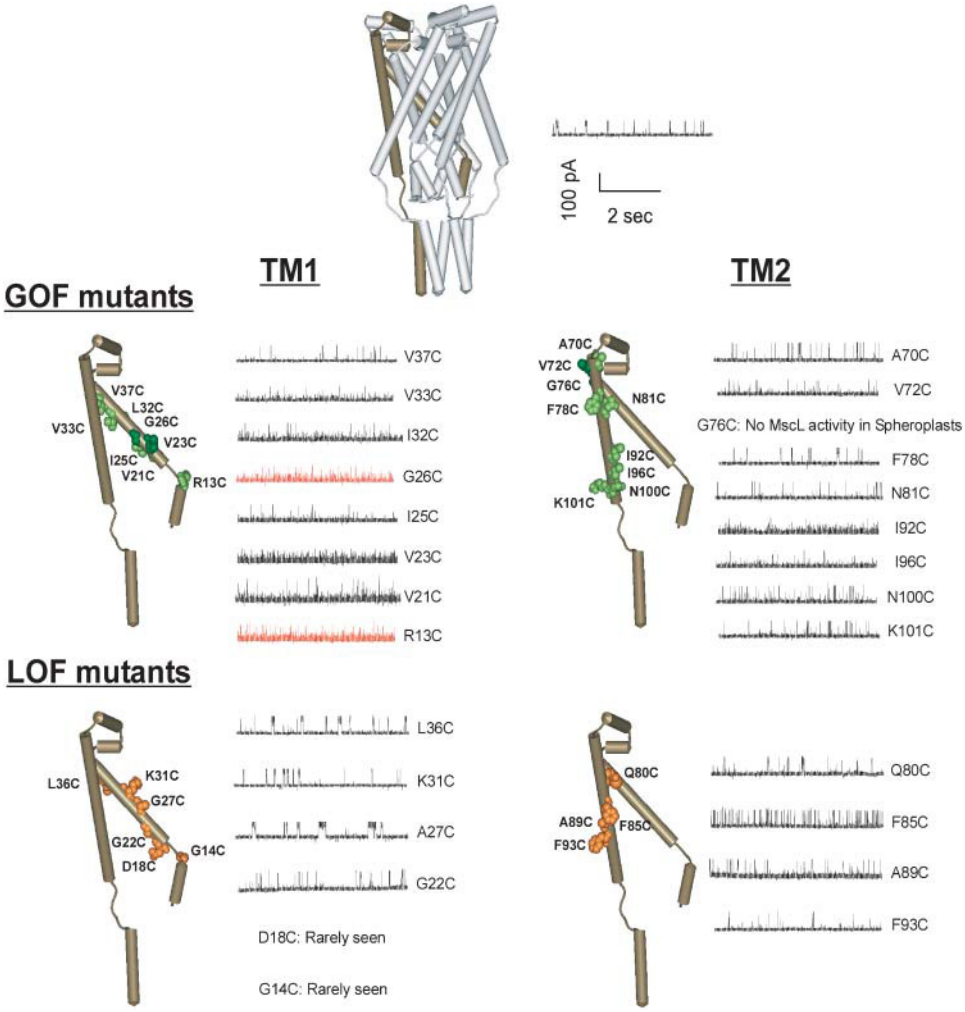

FIGURE 3 Positions and single-channel recording of strong GOF and LOF mutants. A model for the closed *E. coli* MscL channel (Sukharev et al., 2001b), predicted based upon a crystal structure of the *M. tuberculosis* crystal structure (Chang et al., 1998), is used. This complete model and a trace of the wild-type channel are shown (*top*). Cysteine substitutions that led to a strong GOF (*middle*) or LOF (*bottom*) phenotype in vivo are shown in a space-filling model over a single subunit; corresponding channel activities are shown to the right. Residues that induced particularly strong GOF phenotypes are filled with darker green. Traces that were obtained with DTT in the bath are shown in red.

data are largely consistent with our expectations that mutants that do not suppress this phenotype are dysfunctional. In contrast to the GOF mutants (above), these mutants showed no consistency in changes in the open dwell time (compare Tables 1 and 2).

DTT opens channels that are otherwise silent

As mentioned above, three mutations effected GOF phenotypes but were not detected electrophysiologically, even at very high membrane tension. One possible explanation for this apparent paradox is that under highly reduced conditions, as found within living *E. coli* cells (Carmel-Harel and Storz, 2000; Ritz and Beckwith, 2001), the channels open easily; however, when cellular reducing agents such as thioredoxin and glutathione are diluted, as would be expected in an excised patch, they are ''locked'' closed by disulfide bridging. To test if a reducing environment would expose channel activity in these mutants, we treated the patched membranes with 3 mM DTT in the bath. Under these conditions, we observed channel activity for both R13C and G26C (Fig. 4 *A*). In fact, the MscL activities that were revealed had substantially reduced membrane-tension thresholds relative to wild-type. These data are consistent with the channels' ability to effect a GOF phenotype when expressed in the reducing environment of the cell (Fig. 2 *A* and Table 1). MscL activity was revealed in this manner after DTT treatment in all of 10 independent patches of R13C and nine of G26C. In contrast, no activity was observed for G76D, or the LOF mutants G14 and D18, upon DTT addition to either the bath (cytoplasmic side) or the pipette (periplasmic side). DTT also had no effect on MscS or wild-type MscL (not shown).

Biochemical analyses confirm that both R13C and G26C mutants form dimers, even when not subjected to oxidative environments or cross-linking agents. In Fig. 4 *B*, cells were pelleted and lysed immediately upon resuspension in a buffer containing SDS. As discussed above, the bacterial cell is a highly reduced environment. However, even with abrupt cellular lysis and analysis, a significant proportion of the channel subunits is observed as dimers. Treatment of the cell suspension with 100 mM DTT before PAGE fractionation

TABLE 1 Tension sensitivity and kinetics of MscL GOF mutants

	Tension sensitivity	Kinetics	
Strain	Threshold MscL/MscS	τ_2, ms	τ_3, ms
WT	1.55 ± 0.02	9.5 ± 0.8	28 ± 2
TM1			
R13C*	1.11 ± 0.03†	<1	<1
V21C	1.33 ± 0.05	<1	2.6 ± 0.5†
V23C	0.93 ± 0.1†	<1	<1
I25C	1.20 ± 0.06†	1.6 ± 0.3†	3.2 ± 0.3†
G26C*	1.18 ± 0.04†	<1	<1
I32C	1.37 ± 0.05†	<1	<1
V33C	1.30 ± 0.08*	<1	<1
V37C	1.30 ± 0.07*	4.5 ± 0.7†	18 ± 4*
TM2			
A70C	1.77 ± 0.06*	8 ± 1	22 ± 4
V72C	1.77 ± 0.05†	7.4 ± 0.4	39 ± 5
G76C	ND§	ND§	ND§
F78C	1.28 ± 0.03†	0.78 ± 0.08†	2.1 ± 0.2†
N81C	1.42 ± 0.06*	2.3 ± 0.4†	7 ± 1†
I92C	1.22 ± 0.09†	<1	<1
I96C	0.82 ± 0.05†	<1	1.5 ± 0.24†
N100C	0.99 ± 0.05†	1.5 ± 0.4†	7 ± 2†
K101C	0.89 ± 0.07†	2.3 ± 0.5†	2 ± 3†

Pressure threshold was derived using MscS as an internal control as described in Materials and Methods. Values were obtained from at least nine patches that were derived from at least two independent spheroplast preparations. Kinetics were fit assuming three time constants; the shortest (τ_1) is below resolution (~1 ms) and is not presented. Kinetic values were derived from at least 1000 events and two independent spheroplast preparations.

WT, wild-type.

*Values were obtained in the presence of 3–5 mM DTT.

†$p < 0.01$ from WT as determined by Student's *t*-test.

‡$p < 0.05$ from WT as determined by Student's *t*-test.

§Not determined (ND) because activity was not detected.

TABLE 2 Tension sensitivity and kinetics of MscL LOF mutants

	Tension sensitivity	Kinetics	
Strain	Threshold MscL/MscS	τ_2, ms	τ_3, ms
WT	1.55 ± 0.02	9.5 ± 0.8	28 ± 2
TM1			
G14C	ND*	ND*	ND*
D18C	ND*	ND*	ND*
G22C	1.9 ± 0.9†	1.3 ± 0.1†	6 ± 1†
A27C	1.6 ± 0.1	36 ± 9†	127 ± 9†
K31C	1.71 ± 0.07†	13 ± 2‡	35 ± 6
L36C	1.67 ± 0.08‡	15 ± 3‡	58 ± 8†
TM2			
Q80C	2.5 ± 0.2†	1.4§	12.7§
F85C	1.95 ± 0.07†	1.4 ± 0.3†	7 ± 3†
A89C	1.82 ± 0.06†	2.2 ± 0.3†	8.1 ± 0.8†
F93C	2.3 ± 0.1†	<1	3.7§

Pressure threshold was derived using MscS as an internal control as described in Materials and Methods. Values were obtained from at least nine patches that were derived from at least two independent spheroplast preparations. Kinetics were derived from at least 1000 events and two independent spheroplast preparations and fit assuming three time constants; the shortest (τ_1) is below resolution (~1 ms) and is therefore not presented.

WT, wild-type.

*Not determined (ND) because channel activity was not observed often enough for statistical analysis.

†$p < 0.01$ from WT as determined by Student's *t*-test.

‡$p < 0.05$ from WT as determined by Student's *t*-test.

§Values derived from over 250 events, but only on a limited number of patches so statistics are not presented.

caused all detectable MscL subunits to migrate as monomers. Another mutation in TM1, G22C, did not yield dimers under identical conditions, thus demonstrating that dimerization is residue-specific.

DISCUSSION

In this study we use site-directed cysteine scanning to assess the relative importance of residues and subdomains within the transmembrane segments of MscL. Previous studies utilizing random mutagenesis have indicated potential functional regions of the channel. However, interpretation of these studies is often complicated because nonconservative substitutions (e.g., a charge in the middle of a transmembrane domain) can disturb secondary, tertiary, or quaternary structure. Cysteine is a more appropriate substitute for a hydrophobic residue because of the large energetic cost for desolvation of charged residues. Hence, less disruption of conformation of the molecule is anticipated. It also has the advantage that disulfide bridge formation can serve as an indicator of proximity and orientation of residues within the complex. The results obtained help us to evaluate the importance of each residue for normal MscL function. Together, the results support some models for channel gating, while challenging others.

Two opposing models have been proposed for the fundamental gate, or ultimate ion permeation barrier, of the MscL channel. One model proposes that the extreme N-terminal region of the protein, S1, forms the final barrier, or gate, that must open for ion permeation. By this model, the TM1 bundle separates prior to channel gating, yielding a stable ''closed-expanded'' nonconducting state (Sukharev et al., 2001a). This model has been supported primarily by disulfide cross-linking studies. In an alternative model, the TM1 bundle is the primary gate (Blount and Moe, 1999). By this model, the TM1 bundles are tightly packed and permeation is coupled directly and energetically with their separation, not S1's. This latter model is largely supported by mutagenesis studies where it was found that hydrophilic substitutions within this domain led to a GOF phenotype and decreased tension threshold. Essentially all of these mutants had shortened channel open dwell times (Ou et al., 1998; Yoshimura et al., 1999); with some extreme hydrophilic substitutions, substates were stabilized (Yoshimura et al., 1999). One interpretation is that the primary energy barrier for gating is a result of the transient exposure

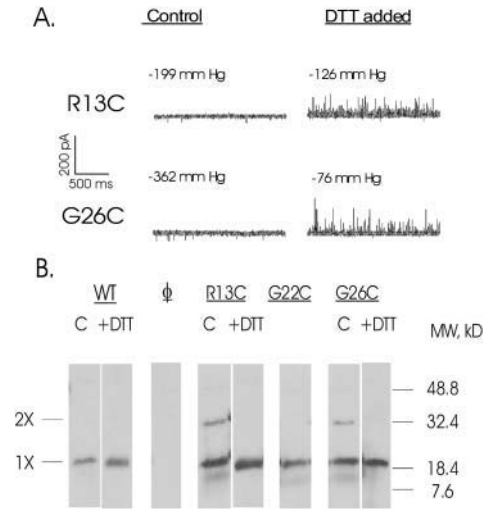

FIGURE 4 Substitutions R13C and G26C spontaneously form disulfide bridges. (*A*) Typical traces of R13C (*top*) and G26C (*bottom*) are shown before (*left*) and after (*right*) addition of 3 mM DTT. The small downward deflections seen in each of the traces are a hallmark of residual MscS channels that do not desensitize and are continuously open at these pressures. Such deflections, also observed in control traces in which no MscL is expressed, appear to be transient closures of MscS. (*B*) Western blot analysis of MscL mutants and controls. Where indicated, the samples were treated with DTT as described in Materials and Methods. The pB10 expression plasmid, not containing *mscL*, is shown as a control (labeled Φ).

of TM1 hydrophobic residues to a more polar environment, presumably the lumen of the pore; hence, transition states are more easily traversed or stabilized by hydrophilic substitutions. This theory was further corroborated in a study in which an engineered cysteine residue at position 22 was chemically modified by sulfhydryl reagents (Yoshimura et al., 2001). Here, we confirm the effect of mutating three of the TM1 residues identified by these mutagenesis studies (R13, V23, and G26) and find further support for the hypothesis by uncovering five additional residues (V21, I25, I32, V33, and V37). Again, with the sole exception of R13, the cysteine substitutions leading to this GOF phenotype are of increased hydrophilicity. In all cases, GOF-generating mutations encode channel activities that have short open dwell times, indicating a lower energy barrier for gating. Note that in the ''closed-expanded'' model, an S1 domain would shield any increased dynamics of TM1 from electrophysiological detection. Hence, the ''flickery'' channel phenotype observed for TM1 mutants strongly suggests ion permeation is directly coupled with TM1 separation.

GOF mutants were also found in TM2. Similar to TM1, most, but not all, of the mutations in this domain that effect an in vivo GOF phenotype encode channel activities that are more sensitive to membrane tension and have shortened open dwell times. One possibility is that the TM2 helix rotates upon gating; thus, similar to TM1, individual residues change their local environment. Indeed, data obtained by site-directed spin-labeling and electron paramagnetic resonance spectroscopy suggest that the TM2 helices rotate in a counterclockwise rotation upon gating (Perozo et al., 2002). However, unlike TM1, here we find little correlation between the GOF phenotype and the hydrophilicity of the substitution, suggesting that other factors (e.g., hydrophobicity or size) may be important at these TM2 sites for maintaining protein-protein or protein-lipid interactions, and thus maintaining a high transition-energy barrier between the closed and open states. Consistent with this hypothesis, portions of this domain face the lipid membrane, and potential interactions with specific lipids have been proposed (Elmore and Dougherty, 2003).

A few mutations within TM2 that are found near the periplasmic region of the helix (A70C, V72C, and G76C) required more, rather than less, tension to gate under patch clamp. At the extreme, G76C activity was not observed. Hence, A70C, V72C, and G76C may effect a GOF phenotype via a solute leak imperceptible in the patch-clamp assay. Alternatively, this region of the protein may interact with some factor missing from patch clamp, such as the large in vivo membrane potential or an auxiliary protein.

Random mutagenesis, coupled with a high throughput assay (Maurer and Dougherty, 2001), has previously been utilized to isolate phenotype-baring mutants (Maurer and Dougherty, 2003). The authors found 32 LOF mutants in 22 residues within the two TM domains of *E. coli*. However, as noted subsequently by the authors (Elmore and Dougherty, 2003), some of the mutants may not simply have deficits in channel gating, but may fail to fold or assemble in the membrane correctly; neither channel activities nor protein expression was presented. Of the 10 LOF mutants identified here, only three overlap with sites found in the previous study; seven are novel. Significantly, all but two of the LOF mutants encoded clearly detectable channel activities that are less sensitive to membrane tension and thus appear to be true LOF mutants, both in vivo and in vitro. Interestingly, the two most severe LOF mutants (G14C and D18C) are near the hypothesized location of the physical gate. Also, it is intriguing that mutation at two of the most conserved phenylalanine residues in TM2, F85 and F93, yields channels that are difficult or impossible to open in vitro. Previous studies have noted that aromatic amino acids are often found at or near the lipid interface (Tsang and Saier, 1996), thus suggesting that one or both of these residues play a key role in determining the location or orientation of the MscL TM2 in one or more of its conformational states.

We have found that in patch clamp, G26C appears to be preferentially locked closed due to disulfide bridging. These data suggest that the G26 residues face each other in a closed conformation. However, the constriction point within the solved crystal structure of the *M. tuberculosis* MscL (Chang et al., 1998) is V21, analogous to V23 in the *E. coli* molecule. Because of the strong homology in this region, it

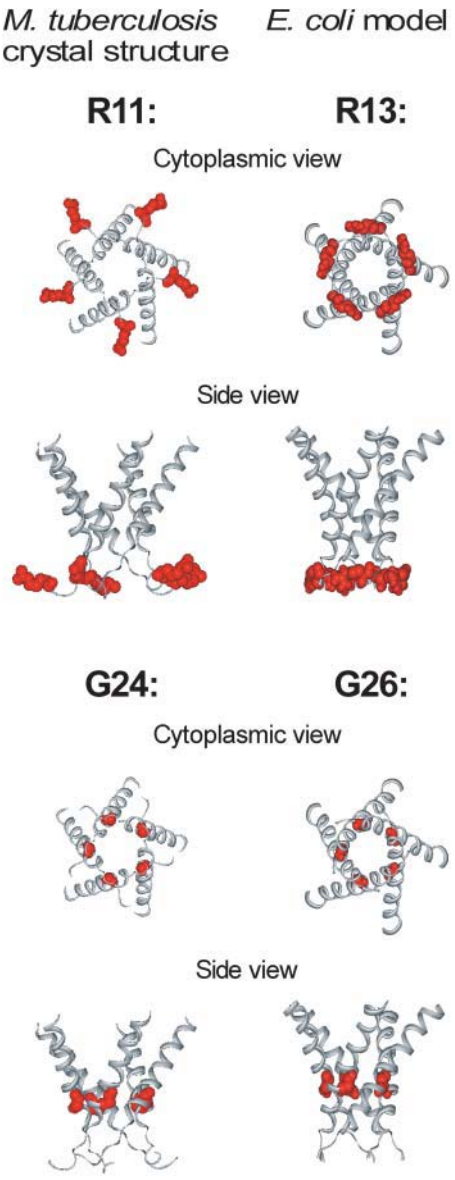

FIGURE 5 R13 and G26 do not face each other in current models for the closed channel of MscL. Neither the crystal structure of the *M. tuberculosis* ortholog (*left*) nor the current model for the *E. coli* closed channel derived from the crystal structure (*right*) predicts that side chains of R13 and G26 (R11 and G24 in *M. tuberculosis*) face the pore. Shown are TM1 domains only (residues 10–40 for the *M. tuberculosis*, 12–42 for *E. coli* MscL).

seems likely that the *M. tuberculosis* and the *E. coli* channels will have the same pore design. Indeed, in both models, the *M. tuberculosis* crystal structure (Chang et al., 1998) and the *E. coli* closed-channel structure derived from it (Sukharev et al., 2001b), the G26 residues (G24 in *M. tuberculosis*) do not face each other (Fig. 5). One interpretation is that disulfide bridging of G26C occurs because of mobility in the region. However, electron paramagnetic resonance spectroscopy demonstrated that this region of the protein is relatively immobile (Perozo et al., 2001). Note also that potential increased mobility upon solubilization is not an issue in these studies because the channel was never removed from its native membrane. The possibility that the GOF properties of G26C increase the mobility of this region cannot be ruled out; however, V23C also effects a GOF phenotype, yet we found no evidence that the V23C channel is locked by disulfide bridges. Perhaps a more likely alternative is that G26 is indeed at the constriction point of a closed state of the channel. If true, then the helix would have to be rotated slightly counterclockwise from what is reported in the crystal structure. Such a rotation would reorient TM1 glycines, which could conceivably permit better packing and closure of the 4-Å pore observed in the crystal structure, thus yielding a fully closed state. This interpretation would support one model that predicts a clockwise rotation of the helix upon channel opening (Perozo et al., 2002), but opposes a model suggesting an anticlockwise rotation of this domain (Sukharev et al., 2001b; Betanzos et al., 2002).

The G26C and R13C mutations both effect a GOF phenotype in vivo (in the reducing environment of the cell) and in vitro (when DTT is added to the patch). In addition, the open dwell times for both mutants are shortened, suggesting a decreased energy barrier between closed and open states. For G26C, it seems likely that the increased sensitivity of the channel is due to the substitution of a larger or slightly more hydrophilic residue at what is normally an area of pore constriction in the closed state, thus decreasing the energy barrier for gating, as discussed above. Similar to G26C, the observation that substitution of R13 to cysteine locks the channel closed, as assayed by patch clamp, suggests that the side chains either face each other or are mobile in the closed pentameric complex. Unfortunately, experimental data are sparse regarding the dynamics of this residue. Structural models also give few clues: in neither the *M. tuberculosis* crystallographic structure nor the derived model for the *E. coli* MscL does this residue face itself (Fig. 5). For R13, in contrast to G26, it seems likely that the native arginine residues, presumably positively charged, would repel each other, leading to a greater distance between them in the wild-type channel relative to the R13C mutant. Hence, perhaps it is the increased ability of this residue to face or approach itself within the complex during gating that results in a decreased energy barrier between closed and open states for R13C, leading to its GOF phenotype.

In summation, this study may help to distinguish between current models for MscL channel gating. The observed change in kinetics upon hydrophilic substitution within TM1 strongly suggests that separation and reclosure of the TM1 constriction, not the S1 bundle, is directly coupled with gating. Similarly, the data presented here can be more easily interpreted if we assume that the structure resolved for the *M. tuberculosis* MscL channel (Chang et al., 1998) represents a nearly closed rather than fully closed conformation, and that channel closure would be coupled with a counterclockwise, rather than clockwise, rotation of TM1.

The authors thank Sharmini Long, Ryan Corley, Robin Wray, and Dr. Yuezhou Li for technical assistance, and Jessica Bartlett and Drs. Paul Moe and Irene Iscla for critical reading of the manuscript.

This work was supported by grants GM61028 and DK60818 from the National Institutes of Health, grant I-1420 of the Welch Foundation, and grant F49620-01-1-0503 of the Air Force Office of Scientific Review.

REFERENCES

Ajouz, B., C. Berrier, A. Garrigues, M. Besnard, and A. Ghazi. 1998. Release of thioredoxin via the mechanosensitive channel MscL during osmotic downshock of *Escherichia coli* cells. *J. Biol. Chem.* 273:26670–26674.

Berrier, C., M. Besnard, B. Ajouz, A. Coulombe, and A. Ghazi. 1996. Multiple mechanosensitive ion channels from *Escherichia coli*, activated at different thresholds of applied pressure. *J. Membr. Biol.* 151:175–187.

Berrier, C., A. Garrigues, G. Richarme, and A. Ghazi. 2000. Elongation factor Tu and DnaK are transferred from the cytoplasm to the periplasm of *Escherichia coli* during osmotic downshock presumably via the mechanosensitive channel *mscL*. *J. Bacteriol.* 182:248–251.

Betanzos, M., C. S. Chiang, H. R. Guy, and S. Sukharev. 2002. A large iris-like expansion of a mechanosensitive channel protein induced by membrane tension. *Nat. Struct. Biol.* 9:704–710.

Blount, P., and P. Moe. 1999. Bacterial mechanosensitive channels: integrating physiology, structure and function. *Trends Microbiol.* 7:420–424.

Blount, P., M. J. Schroeder, and C. Kung. 1997. Mutations in a bacterial mechanosensitive channel change the cellular response to osmotic stress. *J. Biol. Chem.* 272:32150–32157.

Blount, P., S. I. Sukharev, P. C. Moe, B. Martinac, and C. Kung. 1999. Mechanosensitive channels of bacteria. *Methods Enzymol.* 294:458–482.

Blount, P., S. I. Sukharev, P. C. Moe, M. J. Schroeder, H. R. Guy, and C. Kung. 1996a. Membrane topology and multimeric structure of a mechanosensitive channel protein of *Escherichia coli*. *EMBO J.* 15: 4798–4805.

Blount, P., S. I. Sukharev, M. J. Schroeder, S. K. Nagle, and C. Kung. 1996b. Single residue substitutions that change the gating properties of a mechanosensitive channel in *Escherichia coli*. *Proc. Natl. Acad. Sci. USA.* 93:11652–11657.

Carmel-Harel, O., and G. Storz. 2000. Roles of the glutathione- and thioredoxin-dependent reduction systems in the *Escherichia coli* and *Saccharomyces cerevisiae* responses to oxidative stress. *Annu. Rev. Microbiol.* 54:439–461.

Chang, G., R. H. Spencer, A. T. Lee, M. T. Barclay, and D. C. Rees. 1998. Structure of the MscL homolog from *Mycobacterium tuberculosis*: A gated mechanosensitive ion channel. *Science.* 282:2220–2226.

Cruickshank, C. C., R. F. Minchin, A. C. Le Dain, and B. Martinac. 1997. Estimation of the pore size of the large-conductance mechanosensitive ion channel of *Escherichia coli*. *Biophys. J.* 73:1925–1931.

Elmore, D. E., and D. A. Dougherty. 2003. Investigating lipid composition effects on the mechanosensitive channel of large conductance (MscL) using molecular dynamics simulations. *Biophys. J.* 85:1512–1524.

Epstein, W., and M. Davies. 1970. Potassium-dependent mutants of *Escherichia coli* K-12. *J. Bacteriol.* 101:836–843.

Epstein, W., and B. S. Kim. 1971. Potassium transport loci in *Escherichia coli* K-12. *J. Bacteriol.* 108:639–644.

Hamill, O. P., and B. Martinac. 2001. Molecular basis of mechanotransduction in living cells. *Physiol. Rev.* 81:685–740.

Häse, C. C., A. C. Le Dain, and B. Martinac. 1995. Purification and functional reconstitution of the recombinant large mechanosensitive ion channel (MscL) of *Escherichia coli*. *J. Biol. Chem.* 270:18329–18334.

Kumánovics, A., G. Levin, and P. Blount. 2002. Family ties of gated pores: evolution of the sensor module. *FASEB J.* 16:1623–1629.

Lee, G. F., D. P. Dutton, and G. L. Hazelbauer. 1995. Identification of functionally important helical faces in transmembrane segments by scanning mutagenesis. *Proc. Natl. Acad. Sci. USA.* 92:5416–5420.

Levina, N., S. Totemeyer, N. R. Stokes, P. Louis, M. A. Jones, and I. R. Booth. 1999. Protection of *Escherichia coli* cells against extreme turgor by activation of MscS and MscL mechanosensitive channels: identification of genes required for MscS activity. *EMBO J.* 18:1730–1737.

Maurer, J. A., and D. A. Dougherty. 2001. A high-throughput screen for MscL channel activity and mutational phenotyping. *Biochim. Biophys. Acta.* 1514:165–169.

Maurer, J. A., and D. A. Dougherty. 2003. Generation and evaluation of a large mutational library from the *E. coli* mechanosensitive channel of large conductance, MscL. Implications for channel gating and evolutionary design. *J. Biol. Chem.* 278:21076–21082.

Maurer, J. A., D. E. Elmore, H. A. Lester, and D. A. Dougherty. 2000. Comparing and contrasting *Escherichia coli* and *Mycobacterium tuberculosis* mechanosensitive channels (MscL). New gain of function mutations in the loop region. *J. Biol. Chem.* 275:22238–22244.

Moe, P. C., G. Levin, and P. Blount. 2000. Correlating a protein structure with function of a bacterial mechanosensitive channel. *J. Biol. Chem.* 275:31121–31127.

Okada, K., P. C. Moe, and P. Blount. 2002. Functional design of bacterial mechanosensitive channels: Comparisons and contrasts illuminated by random mutagenesis. *J. Biol. Chem.* 277:27682–27688.

Ou, X., P. Blount, R. J. Hoffman, and C. Kung. 1998. One face of a transmembrane helix is crucial in mechanosensitive channel gating. *Proc. Natl. Acad. Sci. USA.* 95:11471–11475.

Perozo, E., D. M. Cortes, P. Sompornpisut, A. Kloda, and B. Martinac. 2002. Open channel structure of MscL and the gating mechanism of mechanosensitive channels. *Nature.* 418:942–948.

Perozo, E., A. Kloda, D. M. Cortes, and B. Martinac. 2001. Site-directed spin-labeling analysis of reconstituted MscL in the closed state. *J. Gen. Physiol.* 118:193–206.

Ritz, D., and J. Beckwith. 2001. Roles of thiol-redox pathways in bacteria. *Annu. Rev. Microbiol.* 55:21–48.

Sukharev, S., M. Betanzos, C. Chiang, and H. Guy. 2001a. The gating mechanism of the large mechanosensitive channel MscL. *Nature.* 409:720–724.

Sukharev, S. I., P. Blount, B. Martinac, F. R. Blattner, and C. Kung. 1994. A large-conductance mechanosensitive channel in *E. coli* encoded by *mscL* alone. *Nature.* 368:265–268.

Sukharev, S., S. R. Durell, and H. R. Guy. 2001b. Structural models of the MscL gating mechanism. *Biophys. J.* 81:917–936.

Tsang, S., and M. H. Saier, Jr. 1996. A simple flexible program for the computational analysis of amino acyl residue distribution in proteins: application to the distribution of aromatic versus aliphatic hydrophobic amino acids in transmembrane alpha-helical spanners of integral membrane transport proteins. *J. Comput. Biol.* 3:185–190.

Yoshimura, K., A. Batiza, and C. Kung. 2001. Chemically charging the pore constriction opens the mechanosensitive channel MscL. *Biophys. J.* 80:2198–2206.

Yoshimura, K., A. Batiza, M. Schroeder, P. Blount, and C. Kung. 1999. Hydrophilicity of a single residue within MscL correlates with increased channel mechanosensitivity. *Biophys. J.* 77:1960–1972.